Environmental Science & Technology

pubs.acs.org/est

Article

Pyrogenic Black Carbon Suppresses Microbial Methane Production by Serving as a Terminal Electron Acceptor

Danhui Xin,[†] Weila Li,[†] Jiwon Choi, Yu-Han Yu, and Pei C. Chiu*

Cite This: *Environ. Sci. Technol.* 2023, 57, 20605−20614

Read Online

ACCESS | Metrics & More | Article Recommendations | Supporting Information

ABSTRACT: Methane (CH_4) is the second most important greenhouse gas, 27 times as potent as CO_2 and responsible for >30% of the current anthropogenic warming. Globally, more than half of CH_4 is produced microbially through methanogenesis. Pyrogenic black carbon possesses a considerable electron storage capacity (ESC) and can be an electron donor or acceptor for abiotic and microbial redox transformation. Using wood-derived biochar as a model black carbon, we demonstrated that air-oxidized black carbon served as an electron acceptor to support anaerobic oxidation of organic substrates, thereby suppressing CH_4 production. Black carbon-respiring bacteria were immediately active and outcompeted methanogens. Significant CH_4 did not form until the bioavailable electron-accepting capacity of the biochar was exhausted. An experiment with labeled acetate ($^{13}CH_3COO^-$) yielded 1:1 $^{13}CH_4$ and $^{12}CO_2$ without biochar and predominantly $^{13}CO_2$ with biochar, indicating that biochar enabled anaerobic acetate oxidation at the expense of methanogenesis. Methanogens were enriched following acetate fermentation but only in the absence of biochar. The electron balance shows that approximately half (~2.4 mmol/g) of biochar's ESC was utilized by the culture, corresponding to the portion of the ESC > +0.173 V (vs SHE). These results provide a mechanistic basis for quantifying the climate impact of black carbon and developing ESC-based applications to reduce CH_4 emissions from biogenic sources.

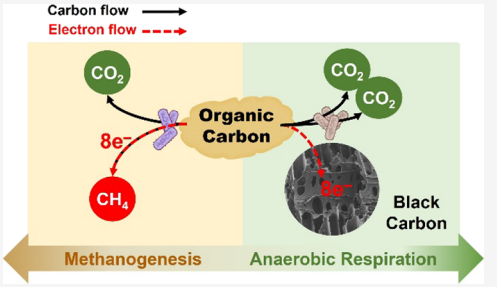

KEYWORDS: *methane, climate, greenhouse gas, black carbon, biochar, electron-accepting capacity, electron storage capacity, methanogenesis, anaerobic respiration*

INTRODUCTION

Methane (CH_4) is the second most important greenhouse gas (GHG),[1,2] contributing to roughly one-third of the current anthropogenic warming.[3] Although its atmospheric concentration is only <0.5% that of CO_2, CH_4 is a far more potent GHG on a mass basis, with a global warming potential (GWP) 27 and 80 times that of CO_2 over 100 and 20 years, respectively.[4−6] In addition, because of its short lifetime (11.8 years[6,7]) in the atmosphere, CH_4 poses an outsized warming effect in the near term.

Conversely, the high warming potency and short lifetime of CH_4 also represent a unique opportunity to rapidly reduce warming. Indeed, of all the short-lived climate forcers, CH_4 has the largest potential for reduction,[8,9] and cutting CH_4 emissions has been recognized as the single most important step that our society can take to reduce the rate of warming and avoid the most disastrous consequences of climate change in the short and medium terms.[10,11] In addition to mitigating global warming, cutting methane emissions also delivers a whole host of other benefits, including lower volatile organic compound (VOC) and ozone concentrations in the troposphere, and hence an improved air quality and public and ecosystem health.

Most global CH_4 emissions come from two types of sources, each contributing approximately half of the total emissions: energy production, such as oil, gas, and coal mining facilities, and anaerobic systems, such as livestock operations, wetlands, rice paddies, solid waste, wastewater, and sludge treatment facilities.[6] For the latter, the source of CH_4 is microbial, and the culprit is methanogens—a group of strictly anaerobic archaea that produce CH_4 from acetate, H_2, and other substrates.[5,12−14] Acetate is fermented to produce equimolar amounts of CH_4 and CO_2 (acetoclastic methanogenesis), whereas H_2 is used to reduce CO_2 to CH_4 (hydrogenotrophic methanogenesis). In both cases, CH_4 is the ultimate electron sink, possessing eight electrons from one molecule of acetate (eq 1) or four molecules of H_2 (eq 2)

$$CH_3COO^- + H^+ = CO_2 + CH_4 \quad (1)$$

Received: July 21, 2023
Revised: November 5, 2023
Accepted: November 13, 2023
Published: December 1, 2023

$$4H_2 + CO_2 = 2H_2O + CH_4 \quad (2)$$

Lower CH_4 emissions have been observed in the presence of a terminal electron acceptor such as sulfate,[15] ferric (oxyhydr)-oxides,[16,17] and humic substances.[18−20] Instead of CH_4 being the electron sink, electrons are transferred by anaerobic bacteria to electron acceptors through respiration, which competes with and suppresses methanogenesis.[21] This suggests that introducing an electron acceptor into a methanogenic system may be a viable strategy to reduce CH_4 emissions.

Pyrogenic black carbon (BC) is produced from biomass through natural and anthropogenic thermal processes such as wildfires and deforestation. Globally, 114−383 million tons (Tg) of BC is produced every year,[22] which represents an integral part of the global carbon cycle. Prior work has shown that BC such as plant-derived biochar and wildfire char possesses sizable and regenerable electron storage capacities (ESCs).[23−27] The ESC of BC is believed to be composed of redox-facile functional groups such as (hydro)quinones,[26] which are created through/during pyrolysis.[23] Conceptually, ESC is the sum of the electron-donating capacity (EDC) and electron-accepting capacity (EAC). However, unlike EDC and EAC, which vary with the redox potential of the system, the ESC of a pyrogenic BC is constant when measured with a given pair of redox titrants.[23] The ESCs of BC derived from plants such as wood and grass and from plant constituents such as cellulose, hemicellulose, and lignin range from 0.5 to 7 mmol/g depending on the source biomass and pyrolysis conditions.[23,24] Through silver tagging and microtomic imaging, it was confirmed that ESC is distributed not only at/near the surface but throughout the interior of BC particles.[25] Studies also showed that microorganisms could partially access these ESC sites.[28,29] For example, the bacterium *Geobacter metallireducens* could access 0.86 mmol/g, or *ca.* 22%, of the ESC of a wood biochar, using it as an electron donor to reduce nitrate when the ESC was electron-filled, or as an electron acceptor to oxidize acetate when the ESC was electron-depleted.[29]

BC such as biochar has been suggested to mitigate GHG production.[30,31] However, exactly how this can occur remains unclear.[32−34] In this study, we demonstrated a specific mechanism through which pyrogenic BC reduces microbial CH_4 production. We postulated that, through its ESC, BC can act as a terminal electron acceptor to enable anaerobic respiration and suppress methanogenesis. That is, electron flow through an anaerobic ecosystem can be diverted to BC instead of to CH_4. We quantified the portion of the ESC that was microbially utilizable in order to establish an electron balance. We also estimated the corresponding minimum reduction potential of the redox moieties in BC that could support anaerobic respiration. In addition, the microbial communities with and without BC were compared through 16S rRNA gene amplicon sequencing and taxonomic analysis. Finally, we offer an estimate of the climate impact of pyrogenic carbon and discuss the potential implications and applications of our findings.

MATERIALS AND METHODS

Chemicals. Solutions of sodium hydroxide (NaOH, 50%) and hydrochloric acid (HCl, 36.5−38%), potassium phosphate dibasic (K_2HPO_4, 99.4%), magnesium chloride hexahydrate ($MgCl_2{\cdot}6H_2O$, >99.0%), calcium chloride dihydrate ($CaCl_2{\cdot}2H_2O$, >99.0%), and potassium chloride (KCl, >99.0%) were purchased from Fisher Scientific (Pittsburgh, PA). Sodium acetate-2-^{13}C ($^{13}CH_3COONa$, 99% ^{13}C atom) and ammonium chloride (NH_4Cl, 99.5%) were obtained from Sigma-Aldrich (St. Louis, MO). Sodium phosphate monobasic dihydrate ($NaH_2PO_4{\cdot}2H_2O$, 99.5%) was acquired from J. T. Baker (Phillipsburg, NJ). Tween 80 (polysorbate 80) was obtained from Acros Organics (Morris Plains, NJ). Vitamin (MD-VS) and trace element (MD-TMS) solutions were purchased from American Type Culture Collection (ATCC, Manassas, VA) for microbial incubation. All chemicals were used as received.

Black Carbon. Soil Reef biochar (SRB), produced through pyrolysis of Southern Yellow wood chips at 550 °C, was used as a model BC. SRB was chosen for the following reasons. (1) It has been used as a reference BC material to study the ESC of a broad spectrum of natural and manmade pyrogenic BC.[23] (2) The size, reversibility,[35] and distribution[25] of SRB's ESC have been determined in previous studies. (3) The physical−chemical properties of SRB have been measured.[27] (4) The percentage of SRB's ESC that is accessible to *G. metallireducens* has been reported.[29] The portion that is accessible to mixed consortia, however, was unknown and was evaluated in this study, as the comparison may provide useful insights into how microbes access black carbon's ESC.

SRB was sieved to the 250−500 μm size fraction and used for all experiments. To eliminate residual electrons (i.e., to oxidize reduced functional groups in SRB) and hence maximize the electron-accepting capacity, SRB was oxidized in continuously aerated, dissolved O_2-saturated deionized water (E_H = +0.80 V vs the standard hydrogen electrode, or SHE, pH 7.0 ± 0.5, P_{O_2}= 0.21 atm) for 10 days. pH of the aerated water was controlled through dropwise addition of H_2SO_4. The oxidized SRB was vacuum-filtered, dried at 60 °C, placed under vacuum overnight, and then transferred to an anaerobic glovebox (Coy Laboratory, Grass Lake, MI) under 98 ± 0.5% N_2 and 2.0 ± 0.5% H_2 (P_{O_2} < 5 ppm). The SRB was stored in the glovebox for 10 days to eliminate any residual sorbed O_2.

Culture. Activated sludge was collected from the secondary treatment tank of Aberdeen Advanced Wastewater Treatment Plant in Aberdeen, MD. The activated sludge had a total suspended solid of 23.27 ± 0.05 g/L, an optical density at 600 nm (OD_{600}) of 1.80, a dissolved organic carbon of 72.2 ± 4.2 mg/L after filtration with a 0.22 μm PVDF filter, and a pH of 6.60 ± 0.17. The sludge was collected in a sealed glass bottle without a headspace and stored at 4 °C. Twenty-four hours prior to use, the sludge was placed in an incubator at 30 °C for preactivation, mixed, and used as a seed culture.

EAC Measurement. The EACs of air-oxidized and deoxygenated SRB and SRB samples collected at the end of an acetate incubation experiment (described below) were measured through chemical redox titration using titanium(III) citrate (−0.36 V vs SHE at pH 6.4) as a reductant, following the method established by Xin et al. (2019)[23,35] Briefly, EAC was determined based on cumulative oxidation of Ti(III) by SRB, as measured by UV−vis absorption at 400 nm. For air-oxidized SRB, the EAC was taken to be the ESC of the SRB for the E_H range of −0.36 to +0.80 V vs SHE; i.e., in the E_H range between the Ti(IV)/Ti(III) and O_2/H_2O redox couples. EAC measurements were repeated using different masses of air-oxidized SRB in duplicate with the control (without SRB) to ensure that the ESC of SRB was constant and independent of the char mass used.

https://doi.org/10.1021/acs.est.3c05830
Environ. Sci. Technol. 2023, 57, 20605−20614

The SRB sample (that had been microbially reduced) retrieved at the end of the acetate experiment was thoroughly washed with Tween 80 before its EAC was measured with Ti(III) citrate. Validation of the washing procedure with Tween 80 is detailed in Section S1 of the Supporting Information. Briefly, microbially reduced SRB was placed in anoxic 1% Tween 80 solution on an orbital shaker at 300 rpm for 20 min to remove cells and biomolecules that were attached to SRB and could potentially bias the EAC measurement. The control showed that the 1% Tween 80 treatment did not alter the measured EAC relative to virgin SRB.

Sludge Incubation Experiment. A sludge incubation experiment was conducted in 155 mL serum bottles. Four sets of reactors were prepared in sextuplicate: with no SRB, 0.5 g of SRB, and 1.0 g of SRB, plus a medium blank (no SRB or sludge). For the first three sets of reactors, each bottle received 48 mL of an aqueous solution consisting of 30 mL of sludge, 12 mL of 4× concentrated basal medium, and 6 mL of deionized water. The blank received 12 mL of a concentrated basal medium and 36 mL of deionized water. The basal medium included 30 mM phosphate buffer to help maintain the solution pH at 6.50 ± 0.30 throughout the incubation and across treatments. The final solution contained 0.400 g/L $MgCl_2{\cdot}6H_2O$, 0.113 g/L $CaCl_2{\cdot}2H_2O$, 0.027 g/L NH_4Cl, 2.971 g/L $KH_2PO_4{\cdot}H_2O$, 1.908 g/L $Na_2HPO_4{\cdot}2H_2O$, 1 mL/L MD-VS vitamin solution, and 1 mL/L MD-TMS trace mineral solution.

All reactors were prepared in an anaerobic glovebox. All solutions except sludge were either autoclaved at 121 °C before being transferred into the glovebox or sterilized using 0.22 μm PTFE filters inside the glovebox. All other materials were autoclaved before use. Each reactor was sealed with a rubber stopper and an aluminum crimp cap, removed from the glovebox, and flushed with high-purity N_2 for 3 min at a flow rate of 7 L/min to remove any H_2 carried over from the glovebox. All reactors were wrapped with aluminum foil and stored in an incubator (Heratherm, Thermo Fisher Scientific, Waltham, MA) at 30 °C for 20 days. Reactors were removed from the incubator at different times, and 50 μL gas samples were withdrawn from the headspace using a gastight syringe and immediately analyzed for CH_4 and CO_2 using a gas chromatograph−mass spectrometer (GC-MS, 6890-5973N, Agilent, Santa Clara, CA). For each sampling event, three reactors were randomly chosen from the sextuplicates for analysis.

^{13}C-Acetate Incubation Experiment. A second incubation experiment was conducted with sodium acetate-2-^{13}C ($^{13}CH_3COONa$) as the main substrate. The same (155 mL) serum bottles were used to prepare five sets of reactors in quadruplicates: with no SRB, 0.5 g of SRB, and 1.0 g of SRB, plus the control (sludge only, no SRB or acetate) and medium blank (no SRB, acetate, or sludge). For the first three sets of reactors, each serum bottle received 60 mL of solution consisting of 3 mL of sludge, 12 mL of 25 mM acetate, 15 mL of 4× concentrated basal medium, and 30 mL of deionized water. For the sludge-only control and medium blank, 12 and 15 mL of deionized water were added, respectively, in place of acetate and sludge. The composition and pH (6.50) of the medium were the same as those in the sludge incubation experiment. All reactors were placed in an incubator at 30 °C for 30 days and sampled at different elapsed times for $^{12}CH_4$, $^{13}CH_4$, $^{12}CO_2$, and $^{13}CO_2$ using a GC-MS.

GC-MS Analysis. Fifty μL of gas sample was withdrawn from the headspace of reactors using a 250 μL gastight syringe equipped with a Mininert valve and a side port needle. The GC-MS was equipped with an Agilent 19091P-QO3 column (15 m × 20 μm) with grade 5 helium as the carrier gas at 1.6 mL/min. The injector and oven temperatures were constant at 250 and 35 °C, respectively. The total run time was 1 min, and the retention times of CH_4 and CO_2 were 0.53 and 0.79 min, respectively.

The MS was run in selective ion monitoring mode. Five ions were monitored for all analyses: m/z = 12, 15, 17, 44, and 45. Gas-phase concentrations of $^{13}CH_4$, $^{12}CH_4$, $^{13}CO_2$, and $^{12}CO_2$ were determined based on total integrated ion abundance: $^{12}CH_4$ was confirmed based on m/z = 12, $^{12}CH_4$ and $^{13}CH_4$ were quantified based on m/z = 15 and 17, and $^{12}CO_2$ and $^{13}CO_2$ were quantified based on m/z = 44 and 45, respectively. Grade 5 $^{12}CH_4$ and $^{12}CO_2$ and 99% ^{13}C purity $^{13}CH_4$ and $^{13}CO_2$ (Millipore Sigma, Burlington, MA) were used as calibration standards. The total masses of CH_4, CO_2, $^{13}CH_4$, and $^{13}CO_2$ in an entire reactor were calculated from the measured headspace concentrations using the Henry's law constants of CH_4 and CO_2 and the pK_as of dissolved CO_2, as described below.

Assuming that the gas and liquid phases were at equilibrium at room temperature, the amount of CH_4 or CO_2 in the aqueous phase ($n_{aqCH_4\ or\ CO_2}$ in mol) can be calculated (eq 3):

$$n_{aq_{CH_4 or CO_2}} = (P_{CH_4 or CO_2}/H_{C_{CH_4 or CO_2}})V_{aq} \quad (3)$$

where H_C is Henry's law constant for CH_4 (714 atm·L/mol) and CO_2 (31.6 atm·L/mol) and V_{aq} is 0.048 L for the sludge experiment and 0.060 L for the acetate experiment.

The total mass of CH_4 in each reactor was thus

$$n_{tot_{CH_4}} = n_{g_{CH_4}} + n_{aq_{CH_4}} \quad (4)$$

The total CO_2 in solution was the sum of dissolved CO_2 (pK_{a1} 6.3), bicarbonate (HCO_3^-, pK_{a2} 10.3), and carbonate (CO_3^{2-}), calculated using eq 5:

$$\begin{aligned} C_{aqtot\_CO_2} &= C_{aqCO_2} + C_{aqHCO_3^-} + C_{aqCO_3^{2-}} \\ &= C_{aqCO_2}[1 + 10^{(pH-pK_{a1})} + 10^{(2pH-pK_{a1}-pK_{a2})}] \\ &= \frac{n_{aqCO_2}}{V_{aq}}[1 + 10^{(pH-pK_{a1})} + 10^{(2pH-pK_{a1}-pK_{a2})}] \end{aligned} \quad (5)$$

where pH is 6.50 for both experiments.

The total mass of CO_2 in each reactor can thus be calculated based on eq 6:

$$n_{tot_{CO_2}} = n_{g_{CO_2}} + n_{aq_{CO_2}}[1 + 10^{(pH-pK_{a1})} + 10^{(2pH-pK_{a1}-pK_{a2})}] \quad (6)$$

Microbial Community Analysis. Aqueous and/or solid (SRB) samples were collected from the seed sludge and the no-SRB and 1g-SRB reactors at the end of an acetate incubation experiment. The samples were sent to the University of Delaware (UD) Sequencing and Genotyping Center for DNA extraction, high-throughput DNA sequencing, and 16S rRNA gene library construction. DNA was extracted using a Zymo Quick-DNA fungal/bacterial miniprep kit (Zymo Research, Irvine, CA). The primer pair 341F

https://doi.org/10.1021/acs.est.3c05830
Environ. Sci. Technol. 2023, 57, 20605−20614

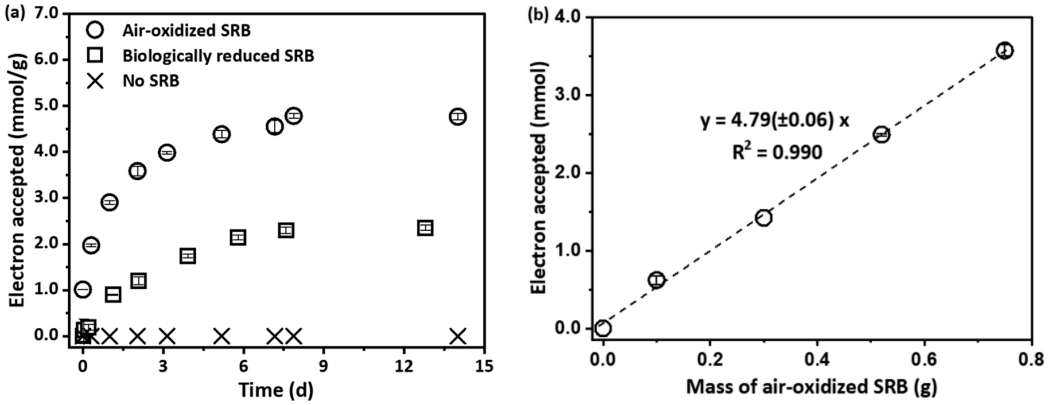

Figure 1. EAC measurement of SRB samples. (a) Cumulative oxidation of Ti(III) citrate by air-oxidized and biologically reduced SRB samples over time. (b) Total amounts of Ti(III) consumed (i.e., electrons transferred) as a function of the SRB mass. Error bars represent the data range from duplicates.

(CCTACGGGNGGCWGCAG)−805R (GACTACHVGGG-TATCTAATCC) was used to target the V3/V4 regions of the 16S rRNA of both bacteria and archaea. Library preparation was performed using a Nextera XT DNA Library Prep Kit (Illumina, San Diego, CA). The Illumina MiSeq platform was used for sequencing the library by 300 base paired-end sequencing. The DNA sequences were then sent to UD Bioinformatics Data Science Core Facility for community analysis using QIIME2 (ver 2023.7).[36] Sequence data was demultiplexed and quality filtered in QIIME2 followed by denoising and clustering of data into amplicon sequence variants performed in DADA2 (ver 1.18.0).[37] Taxonomy was assigned to amplicon sequence variants (ASVs) using QIIME2 classifier against the SILVA database (ver 138).[38]

RESULTS AND DISCUSSION

ESC Measurement. Prior to use in experiments, the ESC of the SRB was measured through chemical redox titration using Ti(III) citrate. As shown in Figure 1a, the total amount of Ti(III) consumed by fully air-oxidized SRB plateaued in *ca.* 8 days and remained constant thereafter, indicating that all its reducible EAC had been filled, i.e., all redox-facile functional groups in SRB that could be reduced by Ti(III) citrate had been reduced. This gives an EAC of 4.81 mmol of electrons per gram, which was taken to be the ESC of the SRB (Figure 1a). Repeating the ESC measurement using different masses of SRB yielded a linear relationship between the SRB mass and total Ti(III) consumed (Figure 1b). The ESC of SRB determined from the slope was 4.79 ± 0.06 mmol/g. Note that it took days for Ti(III) citrate to completely reduce SRB because most of the ESC (i.e., most of the redox-facile functional groups) resides in the interior of the particles[25] and the kinetics of the process was pore diffusion-controlled. We air-oxidized SRB for 10 days for the same reason.[35]

Sludge Experiment. The results of the sludge incubation experiment are shown in Figure 2. In the absence of SRB, organic carbon in the sludge was converted into CO_2 and CH_4 through a combination of fermentation and anaerobic oxidation (Figure 2a). While more CO_2 was produced in early times, similar molar quantities of CO_2 and CH_4 were formed at the end of the 15 day period. A different picture emerged in the presence of 0.5 g of oxidized SRB (Figure 2b): CO_2 appeared immediately and predominated throughout the incubation, suggesting that most of the organic carbon in the

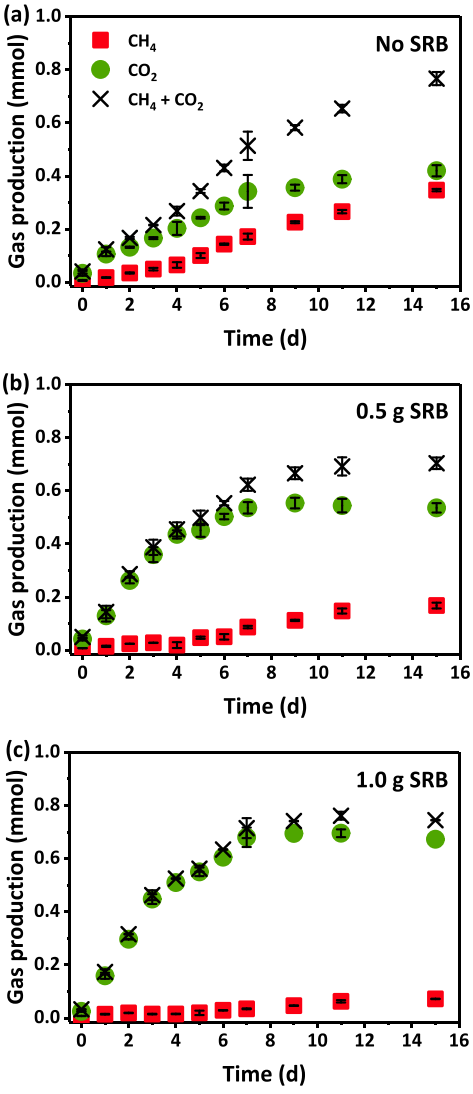

Figure 2. CH_4 and CO_2 production during sludge incubation (a) without SRB, (b) with 0.5 g of oxidized SRB, and (c) with 1.0 g of oxidized SRB. Note that the *y*-axis values represent the total masses of CH_4 and/or CO_2 in the reactors. Error bars represent one standard deviation based on triplicates. No CH_4 or CO_2 was formed in the blank, as shown in Figure S2a.

https://doi.org/10.1021/acs.est.3c05830
Environ. Sci. Technol. 2023, 57, 20605−20614

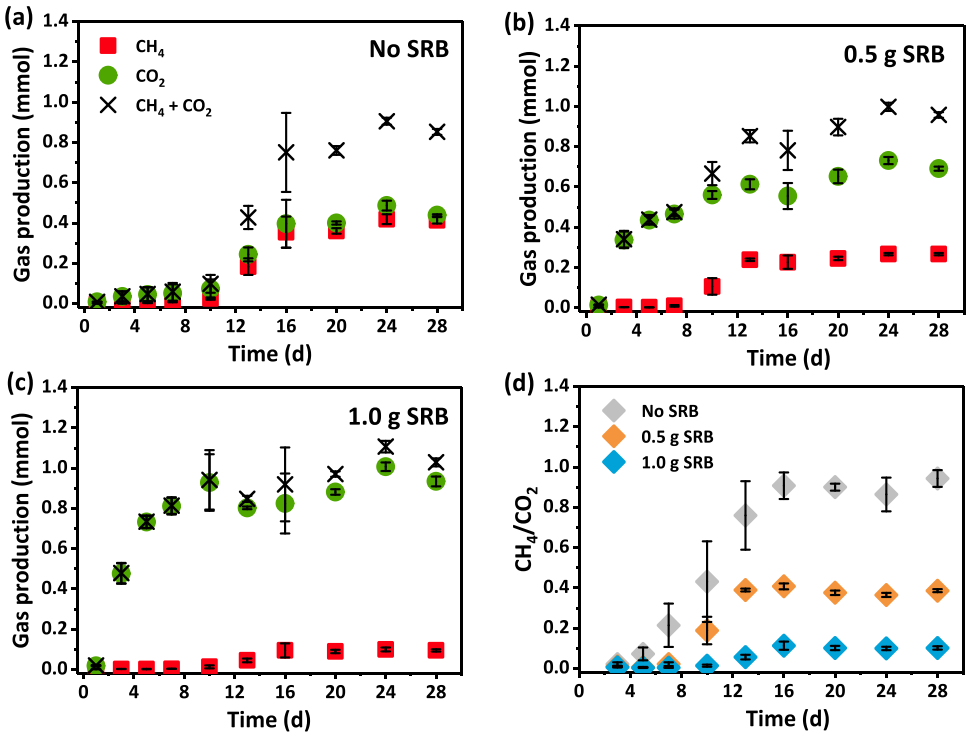

Figure 3. CH_4 and CO_2 production during ^{13}C-labeled acetate ($^{13}CH_3COO^-$) incubation (a) without SRB, (b) with 0.5 g of oxidized SRB, and (c) with 1.0 g of oxidized SRB. The *y*-axis values represent the total masses of CH_4 and/or CO_2 in reactors. (d) The CH_4-to-CO_2 mole ratios were calculated from panels (a) to (c). Error bars represent one standard deviation based on quadruplicates. CH_4 and CO_2 were not formed in the blank and only minimally in the control due to the 5% sludge added, as shown in Figure S2b,c, respectively.

sludge was anaerobically oxidized. CH_4 did not appear until day 5, presumably after the terminal electron acceptors in the system had been largely depleted. The final CH_4 yield was lower by more than 50%, from 0.35 ± 0.004 (Figure 2a) to 0.17 ± 0.01 mmol (Figure 2b). The contrast was even more stark with 1.0 g of SRB (Figure 2c), where CO_2 was almost the exclusive product. CH_4 did not appear until day 9 and accumulated to only 0.07 ± 0.02 mmol.

These results clearly demonstrate that oxidized SRB can suppress methanogenesis, presumably by serving as an electron acceptor to enable anaerobic oxidation of the organic carbon in the sludge. Note that the total gas formed (CH_4 + CO_2) in all reactors at the end of the incubation was relatively constant (0.77 ± 0.05 mmol, Figure 2a–c), indicating that CO_2 was produced at the expense of CH_4. As shown in Figure 2b,c, the microorganisms that respired SRB could do so without a lag, immediately outcompeting the methanogens. Since CH_4 contains all the electrons from acetate or H_2 (eqs 1 and 2), the results suggest that oxidized SRB redirected the electron flow away from methanogenesis by supporting anaerobic oxidation of acetate, H_2, and/or other CH_4 precursors.

Saquing et al. (2016) showed that SRB could serve as a terminal electron acceptor for the oxidation of acetate by *G. metallireducens*.[29] They also reported that each gram of SRB could accept 0.86 mmol of electrons to support acetate oxidation. Our results suggest that the ability to use pyrogenic BC as an electron acceptor is not unique to *G. metallireducens* but is likely common in anaerobic microbial communities. The CO_2 formation data also suggest that the EAC of SRB was readily utilized, and hence, the enzymes involved in BC respiration were presumably constitutive in this culture.

Given the unknown and complex nature of the organic carbon in sludge, it was not possible to establish an electron balance for the data in Figure 2. To that end and to confirm the results of the sludge experiment, we performed another experiment using ^{13}C-labeled acetate ($^{13}CH_3COO^-$) as the predominant substrate/electron donor, with the same sludge as the seed culture (5%, v/v).

Acetate Experiment. Figure 3 shows the results of the acetate incubation experiment. As expected from eq 1, approximately equimolar amounts of CH_4 and CO_2 were produced through acetate fermentation in the absence of SRB (Figure 3a). With 0.5 g of oxidized SRB, CO_2 was the only gas product during the first week and CH_4 did not appear until day 10. For the rest of the incubation, CH_4 and CO_2 were again produced in roughly equimolar quantities (Figure 3b). These results confirm that (1) the microbes in the sludge could use SRB as an electron acceptor for acetate oxidation, (2) the SRB-respiring microorganisms immediately dominated and outcompeted methanogens, and (3) methanogens could start fermenting acetate only after acetate oxidation slowed, presumably because the available EAC of SRB had been largely depleted. With 1.0 g of oxidized SRB, CO_2 was almost the exclusive gaseous product throughout the incubation (Figure 3c), as in the sludge experiment (Figure 2c). CH_4 did not appear until day 13, and its mass never exceeded 0.08 ± 0.01 mmol.

The CH_4-to-CO_2 mole ratios were calculated from Figure 3a–c and used as an indicator of the extent of acetate fermentation (CH_4:CO_2 = 1) relative to the extent of acetate oxidation (CH_4:CO_2 = 0). In the absence of SRB, the increasing CH_4-to-CO_2 ratio in early times and the final value (0.94 ± 0.04) being slightly below 1 suggest the presence of small amounts of electron acceptors (e.g., nitrate) in the wastewater sludge that supported acetate oxidation. With 0.5 and 1.0 g of SRB, the CH_4-to-CO_2 ratio decreased to 0.38 ±

https://doi.org/10.1021/acs.est.3c05830
Environ. Sci. Technol. 2023, 57, 20605−20614

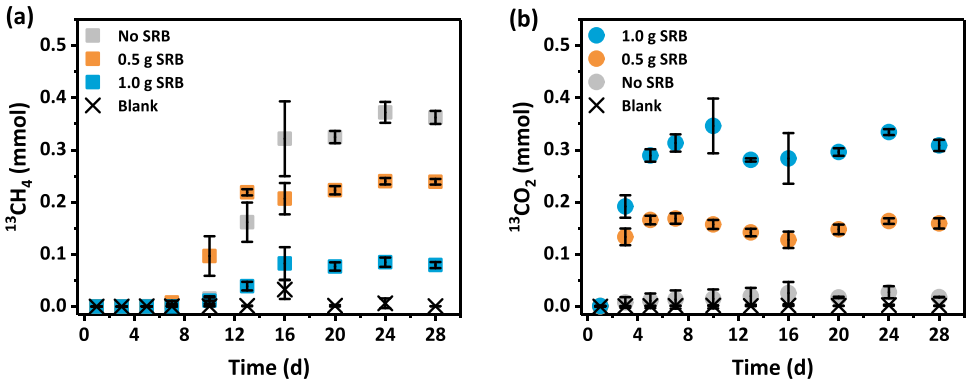

Figure 4. (a) $^{13}CH_4$ and (b) $^{13}CO_2$ production during ^{13}C-labeled acetate incubation with a sludge culture in the presence of 0, 0.5, or 1.0 g of oxidized SRB. The blank contained sludge (5%, v/v) but no SRB or acetate. Error bars represent one standard deviation based on quadruplicates.

0.01 and 0.10 ± 0.01, respectively, clearly indicating shifts in electron flow from acetate fermentation to anaerobic oxidation.

The result of the 16S rRNA gene amplicon sequencing analysis is consistent with the chemical data in Figure 3 and supports the CH_4-suppressing role of SRB. Figure S3 shows the domain- and order-level relative abundance of the microbial communities, as well as the genus-level relative abundance of the archaeal communities, in the seed sludge and in acetate reactors with and without SRB. As shown in Figure S3a, the sludge collected from the aeration basin contained few archaea (and hence few methanogens). The archaeal relative abundance grew markedly from 0.076 to 5.323% after fermentation of acetate to CH_4 and CO_2 (Figure 3a) by acetoclastic methanogens. In contrast, in the presence of 1.0 g of oxidized SRB, archaeal abundance increased negligibly in both the liquid and solid phases, consistent with minimal CH_4 production and dominant acetate oxidation to CO_2 (Figure 3c). The increase in archaeal relative abundance in the absence of SRB was accounted for almost entirely by *Methanosarciniales* (2.408%) and *Methanobacteriales* (2.748%), with *Methanomassiliicoccales*, *Methanofastidiosale*, and *Methanomicrobiales* contributing to the rest (0.167%) (Figure S3b). With 1.0 g of SRB, again, little increase in methanogen abundance was observed except for that of *Methanosarciniales*, which increased from 0.016 to 0.4% in the liquid phase. A few orders of bacteria (e.g., *Spirochaetales* and *Geobacterales*) exhibited a marked increase in relative abundance due to SRB addition. These organisms are candidates for future studies as they may be involved in the (direct or indirect) respiration of black carbon.

The formation of ^{13}C-labeled gases provides further insights into the fate of acetate (Figure 4). Since only the methyl carbon of acetate was ^{13}C-labeled, virtually all CH_4 and CO_2 produced in the absence of SRB were $^{13}CH_4$ (Figure 4a) and $^{12}CO_2$, according to eq 7. Traces of $^{13}CO_2$ were formed (Figure 4b) via acetate oxidation due to small amounts of electron acceptors in the sludge, as noted earlier. With 0.5 and 1.0 g of SRB, production of $^{13}CH_4$ decreased (Figure 4a) and correspondingly the amounts of $^{13}CO_2$ produced increased (Figure 4b), as shown in eq 8. These results support that, as an electron acceptor, SRB shifted the major acetate degradation pathway from fermentation to respiration (of SRB). The amount of $^{13}CO_2$ produced thus represents the electrons diverted to, and the amount of $^{13}CH_4$ formation prevented by, SRB.

$$^{13}CH_3COOH \rightarrow {}^{13}CH_4 + {}^{12}CO_2 \quad (7)$$

$$^{13}CH_3COOH + 8C{=}O_{(\text{quinone in SRB})} + 2H_2O \rightarrow 8C{-}OH_{(\text{hydroquinone in SRB})} + {}^{13}CO_2 + {}^{12}CO_2 \quad (8)$$

$$^{13}CH_3COOH + 2H_2O \rightarrow {}^{13}CO_2 + {}^{12}CO_2 + 8e^- + 8H^+ \quad (8a)$$

$$8C{=}O_{(\text{quinone in SRB})} + 8e^- + 8H^+ \rightarrow 8C{-}OH_{(\text{hydroquinone in SRB})} \quad (8b)$$

To confirm that in both experiments (Figures 2 and 3), SRB prevented CH_4 production rather than enabling CH_4 oxidation after it was produced, we conducted an additional experiment using $^{13}CH_4$ as a substrate under the same conditions as for the acetate experiment. As shown in Figure S4, neither $^{13}CH_4$ consumption nor $^{13}CO_2$ production occurred for 15 days. This confirms that $^{13}CH_3COO^-$ and other organic carbons in the sludge were directly oxidized by SRB respirers, which deprived methanogens of available substrates. CH_4-oxidizing BC-respirers, if existed, were either dormant or few in this culture.

The EAC of SRB that was utilized by the sludge culture can be estimated from the data in Figure 4. With increasing SRB mass, the $^{13}CH_4$ yield decreased from 0.36 ± 0.04 to 0.23 ± 0.02 and then 0.08 ± 0.02 mmol, whereas the $^{13}CO_2$ yield increased from 0.02 ± 0.01 to 0.15 ± 0.02 and then 0.31 ± 0.03 mmol. Hence, the available EAC in 1.0 g of oxidized SRB converted 0.28 ± 0.03 mmol of CH_4 into CO_2. Given that eight electrons are involved in oxidizing CH_4 to CO_2, the EAC of SRB utilized by the culture was 2.24 ± 0.24 mmol/g. Also, given that the total ESC of the SRB was 4.79 mmol/g, approximately half (47 ± 5%) of this capacity was utilized by the sludge culture for acetate oxidation.

To confirm this result and to close the electron balance, SRB samples were collected at the end of the acetate incubation experiment, treated with anoxic Tween 80 solution, and subjected to EAC analysis. As shown in Figure 1a, the "used" SRB recovered from the acetate incubation had an EAC of only 2.31 mmol/g, indicating that it had been partially reduced, i.e., it had accepted 2.48 (= 4.79−2.31) mmol/g of electrons during acetate oxidation. This value of "extra" electrons agrees with that (2.24 mmol/g) associated with the observed decrease in $^{13}CH_4$ and the increase in $^{13}CO_2$. This value also closely matches the electrons associated with the CH_4 decrease and the CO_2 increase in the sludge incubation experiment (Figure 2). These results thus support that (1) the total ESC of this SRB was constant and that (2) as an electron

https://doi.org/10.1021/acs.est.3c05830
Environ. Sci. Technol. 2023, 57, 20605−20614

acceptor, oxidized SRB could divert 2.2−2.5 mmol/g of electrons away from methanogenesis, preventing formation of *ca.* 0.3 mmol of CH_4 per gram of SRB. This capacity appears to be constant in our experiments, regardless of whether the electron donor was acetate or mixed substrates in the sludge. However, if the microbially usable portion of the ESC is thermodynamically controlled (discussed below), the capacity to prevent CH_4 formation should vary with the electron donor, i.e., a higher percentage of the ESC should become available when a thermodynamically stronger electron donor is utilized.

To assess how the portion of microbially usable ESC was controlled, we performed thermodynamic calculations (Section S2, Supporting Information) to estimate the reduction potential of the hypothetical quinone group in SRB that, when serving as an electron acceptor, would render acetate oxidation equally favorable to acetoclastic methanogenesis near the end of the acetate incubation experiment. Our calculations yielded a threshold potential of +0.173 V vs SHE, above which acetate oxidation would be thermodynamically more favorable than methanogenesis. This result suggests that the reason why only ∼50% of the total ESC (4.79 mmol/g) was utilized by the sludge culture is that for only half of the ESC (the half with an E_H > 0.173 V) was acetate oxidation more favorable than fermentation. Once this portion of the ESC was depleted, methanogenesis would commence.

Finally, to assess whether the ability of BC to suppress CH_4 production was unique to SRB, another type of wood char (Rogue biochar, White City, OR) produced by gasification was used for the acetate incubation experiment. The physical−chemical properties of Rogue biochar can be found in Xin et al. (2022).[27] As shown in Figure S5, the same result was obtained as those in Figure 3: acetate was fermented to CH_4 and CO_2 in the absence of biochar, whereas CH_4 was completely suppressed by 1.0 g of oxidized Rogue biochar and CO_2 was the only gas product throughout the incubation. This result suggests that the ability to support anaerobic respiration and suppress methanogenesis may be common to wood-based BC. We previously showed that pyrogenic BC derived from plants and plant polymers, including commercial biochars, laboratory-prepared chars, field-aged chars, and wildfire chars, all possessed sizable ESCs.[23] It is perceivable that all BC possessing ESC can alter microbial GHG composition and hence the climate through the same mechanism as shown in this work, though additional studies are necessary to test this hypothesis.

The bacterium *G. metallireducens* was reported to utilize only ∼22% of the total ESC of SRB (same size fraction, 250−500 μm).[29] The much larger percentage of the ESC utilized in this work suggests that the mixed culture was able to access a larger portion of the redox-labile functional groups (i.e., ESC sites), potentially including those residing in the interior pores of SRB particles.[25] This most likely occurred through the actions of molecular electron shuttles such as flavins, quinones, and/or dissolved organic matter that were either present in the sludge or excreted by the microbes.[39−42] Through pore diffusion, these redox mediators could provide microbes access to the EAC residing in the inner pores of SRB, similar to how they enable microbes to indirectly respire distant solids such as iron and manganese oxides.[39−41] However, further studies with pure strains or specific electron shuttles are necessary to elucidate the mechanism(s) through which microbes deposit and retrieve electrons into and from black carbon.

Many studies have suggested that biochar may affect GHG production; however, the results have been inconsistent or qualitative at best.[30−34,43−45] This is to a large measure due to lack of a clear and testable mechanistic hypothesis for how black carbon exerts its influence. In the mid-2010s, Lovley et al. published a series of papers[46−49] proposing that BC, including graphite, activated carbon, and biochar, promoted microbial CH_4 production. Unaware of ESC,[26] its accessibility to microbes,[29] or the redox state and electron content of the BC that they used, these authors attributed their results solely to BC's electrical conductivity, even though biochar and activated carbon are poorly conductive relative to graphite.[47−49] Our work provides an alternative/additional mechanism and explanation for those earlier studies. In 2021, Sun et al. presented the first clear evidence that addition of BC to anaerobic soil decreased CH_4 production.[32] It would be instructive to compare their study to this work. The results of Sun et al., while convincing, are not quantitative for two reasons. First, the ESC and electron contents of BC used were not controlled or measured. Second, their microcosms contained a significant amount of soil organic matter, which, like BC, possesses abundant redox moieties and can act as an electron acceptor.[20,50] This clouds the contribution of BC. These issues were rectified in this study through (1) ESC/EAC measurements before and after the experiment to establish electron balance, (2) use of ^{13}C-labeled acetate to obtain carbon balance and (3) control of the total EAC in each experiment. This enabled us to quantify the mass of CH_4 diverted per unit mass of BC per redox cycle. Sun et al. attributed the lower CH_4 yields to three possible mechanisms: capacitive, conductive, and redox cycling, although the contribution of each was unclear. Our results show that CH_4 suppression can be attributed to a single mechanism: reversible exchange and storage of electrons in biochar through reactions of its redox functional groups (i.e., ESC). Note that electrons are transferred with protons (eq 8b), and hence, electron storage does not involve charge accumulation. The other mechanisms are unlikely since, in contrast to graphite and nanocarbons, low-temperature plant-based chars are poor electrical conductors and do not accumulate charge like capacitors do.

Environmental Implications. Degradation of organic carbon in anaerobic environments leads to the production of two major GHGs, CO_2 and CH_4, collectively contributing to the majority of anthropogenic warming.[7,51] Due to its high GWP and short atmospheric lifetime, CH_4 exerts an outsized impact on the climate, particularly in the near and medium terms. In this study, we demonstrated the ability of BC to prevent microbial CH_4 production and determined the capacity of a wood biochar (0.3 mmol of CH_4/g) to do so. Using this capacity and the GWP of CH_4 (27.0 and 79.7 over 100 and 20 years, respectively),[6,52] the potential effect of SRB to reduce global warming can be calculated and expressed as CO_2 equivalent (CO_2e) using eq 9

$$CO_2e = m_{CO_2} + m_{CH_4} \times GWP_{CH_4} \quad (9)$$

where m_{CO_2} and m_{CH_4} are the masses of CO_2 and CH_4 produced in each experiment and CO_2e is the mass of CO_2 that would cause the same extent of warming as m_{CO_2} and m_{CH_4} combined.

As shown in Table 1, up to 5.04 kg of CH_4 production may be prevented per ton of SRB based on the acetate experiment.

https://doi.org/10.1021/acs.est.3c05830
Environ. Sci. Technol. 2023, 57, 20605−20614

Table 1. Impact of Biochar on CH_4 and CO_2e over 100 and 20 Years, Estimated Using Data from the Sludge and Acetate Experiments[a]

mg/g SRB (kg/ton SRB)	ΔCH_4	ΔCO_2	ΔCO_2e (100 years)	ΔCO_2e (20 years)
sludge experiment	−4.67	+21.17	−105	−351
^{13}C-acetate experiment	−5.04	+9.96	−126	−392

[a]Total $CO_2e = \Sigma$(GHG mass × GWP) (eq 9). CO_2e was calculated from the differences between biochar-free and biochar-amended samples.

This translates to a reduction of 126 and 392 kg of CO_2e per ton of SRB over a 100 and 20 year time frame, respectively.

Given that wildfires and deforestation convert up to 27% of the biomass into BC and produce >100 Tg of BC annually,[53,54] the amount of CH_4 prevented by BC could be as high as 0.5 million tons per year. This calculation, while preliminary, suggests that the impact of BC as an electron acceptor on the composition of global GHG emitted from microbial sources could be significant. In addition, this calculation considers the effect in only one redox cycle. Previous studies have shown that the EAC of BC is highly regenerable by dissolved O_2 over multiple redox cycles.[23,35] In environments of oscillating redox potential (e.g., wetlands, tidal marshes, rice paddies, etc.), CH_4 suppression by BC may occur continually over repeated redox cycles through periodic regeneration of the EAC by O_2, potentially magnifying the cumulative impact of BC's ESC on the climate.

In addition to the mechanistic explanation and climate implications, this study also provides data for developing potential ESC-based applications for mitigating biogenic CH_4 emissions from natural and anthropogenic sources. A persistent form of carbon, BC such as biochar made from surplus biomass has been proposed as a means to sequester carbon in soil and sediment.[55,56] If engineered properly, BC may also offer the additional benefit of cutting CH_4 emissions. While further studies are necessary, a BC-based technology that includes both carbon stabilization/storage and CH_4 reduction may represent an economically attractive approach to offset carbon emissions or generate carbon credit.

Finally, if BC represents a large, ubiquitous, rechargeable, and microbially accessible electron reservoir, it may affect not only CH_4 but potentially other biogenic GHG, such as nitrous oxide (N_2O). While many studies have tested the effects of BC on nitrification and denitrification, the role of ESC was never considered or understood. Similar to how SRB shifted the electron flow through the sludge microbial community, BC may influence the nitrification and/or denitrification cycles in soil and sediment through its ESC. Given that BC is abundantly produced and ubiquitous, and that ESC is a universal property of plant-based BC,[23] the role and impacts of BC on climate,[57] contaminant fate, biogeochemistry, and other areas of environmental science and engineering need to be better understood. This is particularly vital, given that wildfires are projected to increase in frequency, duration, and intensity in the foreseeable future.

■ ASSOCIATED CONTENT

Data Availability Statement

DNA sequences are available at the National Center for Biotechnology Information (NCBI), BioProject number PRJNA1033353.

Supporting Information

The Supporting Information is available free of charge at https://pubs.acs.org/doi/10.1021/acs.est.3c05830.

Method for washing microbially reduced SRB, thermodynamic calculations for methanogenesis and black carbon respiration, figures showing EAC of differently treated microbially reduced SRB, blanks and controls of sludge and acetate experiments, heatmaps of relative microbial abundance, degradability of $^{13}CH_4$ with oxidized SRB, and acetate incubation experiments with Rogue biochar (PDF)

■ AUTHOR INFORMATION

Corresponding Author

Pei C. Chiu − *Department of Civil and Environmental Engineering, University of Delaware, Newark, Delaware 19716, United States;* orcid.org/0000-0003-2319-4496; Email: pei@udel.edu

Authors

Danhui Xin − *Department of Civil and Environmental Engineering, University of Delaware, Newark, Delaware 19716, United States;* orcid.org/0000-0002-5267-9727

Weila Li − *Department of Civil and Environmental Engineering, University of Delaware, Newark, Delaware 19716, United States*

Jiwon Choi − *Department of Civil and Environmental Engineering, University of Delaware, Newark, Delaware 19716, United States*

Yu-Han Yu − *Department of Civil and Environmental Engineering, University of Delaware, Newark, Delaware 19716, United States*

Complete contact information is available at: https://pubs.acs.org/10.1021/acs.est.3c05830

Author Contributions

†W.L. and D.X. contributed equally to this work.

Notes

The authors declare no competing financial interest.

■ ACKNOWLEDGMENTS

The authors gratefully acknowledge support from the Mid-Atlantic States Section of the Air and Waste Management Association (MASS-A&WMA) through the Air Pollution Educational and Research Grant Program (APERG) for D.X. and funding from University of Delaware's Graduate College through the Interdisciplinary Frontier Graduate and Post-doctoral Fellowship for W.L. We thank Brewster Kingham from the UD Sequencing and Genotyping Center for DNA extraction, sequence library preparation, and 16S sequencing and Shawn W. Polson from UD Bioinformatics Data Science Core Facility for the taxonomic analysis. The 16S rRNA gene amplicon sequencing utilized infrastructure purchased by and analysis services developed with support from Delaware INBRE (NIH P20 GM103446), the State of Delaware, and Delaware Biotechnology Institute. We also thank Heidi Bumba

and Amanda Lo from the Aberdeen Advanced Wastewater Treatment Plant for providing wastewater sludge for this work.

REFERENCES

(1) U.S. EPA. *Overview of Greenhouse Gases*; https://www.epa.gov/ghgemissions/overview-greenhouse-gases.
(2) U.S. EPA. *Methane Emissions and Mitigation Opportunities*. https://www.epa.gov/sites/default/files/2016-04/documents/mon6methaneemissionssourcesgmi.pdf.
(3) *Climate dashboard*; https://www.climatelevels.org/?pid=2degreesinstitute&theme=grid-light (accessed 2023-04−11).
(4) Aronson, E. L.; Allison, S. D.; Helliker, B. R. Environmental Impacts on the Diversity of Methane-Cycling Microbes and Their Resultant Function. *Frontiers in Microbiology. Frontiers Research Foundation* **2013**, *4*, 225.
(5) Nazaries, L.; Murrell, J. C.; Millard, P.; Baggs, L.; Singh, B. K. Methane, Microbes and Models: Fundamental Understanding of the Soil Methane Cycle for Future Predictions. *Environmental Microbiology* **2013**, *15*, 2395−2417.
(6) Forster, P.; Storelvmo, T.; Armour, K.; Collins, W.; Dufresne, J.-L.; Frame, D.; Lunt, D. J.; Mauritsen, T.; Palmer, M. D.; Watanabe, M.; Wild, M.; Zhang, H. The Earth's Energy Budget, Climate Feedbacks, and Climate Sensitivity. In *Climate Change 2021: The Physical Science Basis. Contribution of Working Group I to the Sixth Assessment Report of the Intergovernmental Panel on Climate Change*; Masson-Delmotte, V.; Zhai, P.; Pirani, A.; Connors, S.L.; Péan, C.; Berger, S.; Caud, N.; Chen, Y.; Goldfarb, L.; Gomis, M. I.; Huang, M.; Leitzell, K.; Lonnoy, E.; Matthews, J. B. R.; Maycock, T. K.; Waterfield, T.; Yelekçi, O.; Yu, R.; Zhou, B., Eds.; Cambridge University Press: Cambridge, United Kingdom and New York, NY, USA, 2021: pp 923−1054, DOI: 10.1017/9781009157896.009.
(7) IEA. *Global Methane Tracker 2022*; IEA: Paris, 2022. https://www.iea.org/reports/global-methane-tracker-2022, License: CC BY 4.0.
(8) Stolaroff, J. K.; Bhattacharyya, S.; Smith, C. A.; Bourcier, W. L.; Cameron-Smith, P. J.; Aines, R. D. Review of Methane Mitigation Technologies with Application to Rapid Release of Methane from the Arctic. *Environmental Science & Technology*. **2012**, *46*, 6455−6469.
(9) Sawyer, W.; Genina, I.; Brenneis, R.; Feng, H.; Li, Y.; Lennon Luo, S.-X. Methane Emissions and Global Warming: Mitigation Technologies, Policy Ambitions, and Global Efforts. *MIT Science Policy Review* **2022**, *3*, 73−84.
(10) Hamdan, L. J.; Wickland, K. P. Methane Emissions from Oceans, Coasts, and Freshwater Habitats: New Perspectives and Feedbacks on Climate. *Limnology and Oceanography* **2016**, *61* (S1), S3−S12.
(11) Roth, F.; Broman, E.; Sun, X.; Bonaglia, S.; Nascimento, F.; Prytherch, J.; Brüchert, V.; Zara, M. L.; Brunberg, M.; Geibel, M. C.; Humborg, C.; Norkko, A. Methane Emissions Offset Atmospheric Carbon Dioxide Uptake in Coastal Macroalgae, Mixed Vegetation and Sediment Ecosystems. *Nat. Commun.* **2023**, *14* (1), 42 DOI: 10.1038/s41467-022-35673-9.
(12) Cadena, S.; Cervantes, F. J.; Falcón, L. I.; García-Maldonado, J. Q. The Role of Microorganisms in the Methane Cycle. *Diversity Microb. World* **2019**, *51*, 133 DOI: 10.3389/frym.2019.00133.
(13) Conrad, R. The Global Methane Cycle: Recent Advances in Understanding the Microbial Processes Involved. *Environmental Microbiology Reports* **2009**, *1*, 285−292.
(14) Reeburgh, W. S. Oceanic Methane Biogeochemistry. *Chem. Rev.* **2007**, *38* (20), 486−513.
(15) van Zijderveld, S. M.; Gerrits, W. J. J.; Apajalahti, J. A.; Newbold, J. R.; Dijkstra, J.; Leng, R. A.; Perdok, H. B. Nitrate and Sulfate: Effective Alternative Hydrogen Sinks for Mitigation of Ruminal Methane Production in Sheep. *J. Dairy Sci.* **2010**, *93* (12), 5856−5866.
(16) Van Bodegom, P. M.; Scholten, J. C. M.; Stams, A. J. M. Direct Inhibition of Methanogenesis by Ferric Iron. *FEMS Microbiol. Ecol.* **2004**, *49* (2), 261−268.
(17) Aeppli, M.; Schladow, G.; Lezama Pacheco, J. S.; Fendorf, S. Iron Reduction in Profundal Sediments of Ultraoligotrophic Lake Tahoe under Oxygen-Limited Conditions. *Environ. Sci. Technol.* **2023**, *57* (3), 1529−1537.
(18) Valenzuela, E. I.; Cervantes, F. J. The Role of Humic Substances in Mitigating Greenhouse Gases Emissions: Current Knowledge and Research Gaps. *Sci. Total Environ.* **2021**, *750*, No. 141677.
(19) Blodau, C.; Deppe, M. Humic Acid Addition Lowers Methane Release in Peats of the Mer Bleue Bog, Canada. *Soil Biol. Biochem* **2012**, *52*, 96−98.
(20) Gao, C.; Sander, M.; Agethen, S.; Knorr, K. H. Electron Accepting Capacity of Dissolved and Particulate Organic Matter Control CO_2 and CH_4 Formation in Peat Soils. *Geochim. Cosmochim. Acta* **2019**, *245*, 266−277.
(21) Roden, E. E.; Wetzel, R. G. Organic Carbon Oxidation and Suppression of Methane Production by Microbial Fe(III) Oxide Reduction in Vegetated and Unvegetated Freshwater Wetland Sediments. *Limnol Oceanogr* **1996**, *41* (8), 1733−1748.
(22) Coppola, A. I.; Wiedemeier, D. B.; Galy, V.; Haghipour, N.; Hanke, U. M.; Nascimento, G. S.; Usman, M.; Blattmann, T. M.; Reisser, M.; Freymond, C. V.; Zhao, M.; Voss, B.; Wacker, L.; Schefuß, E.; Peucker-Ehrenbrink, B.; Abiven, S.; Schmidt, M. W. I.; Eglinton, T. I. Global-Scale Evidence for the Refractory Nature of Riverine Black Carbon. *Nat. Geosci* **2018**, *11* (8), 584−588.
(23) Xin, D.; Saha, N.; Reza, M. T.; Hudson, J.; Chiu, P. C. Pyrolysis Creates Electron Storage Capacity of Black Carbon (Biochar) from Lignocellulosic Biomass. *ACS Sustain Chem. Eng.* **2021**, *9* (19), 6821−6831.
(24) Saha, N.; Xin, D.; Chiu, P. C.; Reza, M. T. Effect of Pyrolysis Temperature on Acidic Oxygen-Containing Functional Groups and Electron Storage Capacities of Pyrolyzed Hydrochars. *ACS Sustain Chem. Eng.* **2019**, *7* (9), 8387−8396.
(25) Xin, D.; Barkley, T.; Chiu, P. C. Visualizing Electron Storage Capacity Distribution in Biochar through Silver Tagging. *Chemosphere* **2020**, *248*, No. 125952.
(26) Klüpfel, L.; Keiluweit, M.; Kleber, M.; Sander, M. Redox Properties of Plant Biomass-Derived Black Carbon (Biochar). *Environ. Sci. Technol.* **2014**, *48* (10), 5601−5611.
(27) Xin, D.; Girón, J.; Fuller, M. E.; Chiu, P. C. Abiotic Reduction of 3-Nitro-1,2,4-Triazol-5-One (NTO) and Other Munitions Constituents by Wood-Derived Biochar through Its Rechargeable Electron Storage Capacity. *Environ. Sci. Process Impacts* **2022**, *24* (2), 316−329.
(28) Xu, S.; Adhikari, D.; Huang, R.; Zhang, H.; Tang, Y.; Roden, E.; Yang, Y. Biochar-Facilitated Microbial Reduction of Hematite. *Environ. Sci. Technol.* **2016**, *50* (5), 2389−2395.
(29) Saquing, J. M.; Yu, Y. H.; Chiu, P. C. Wood-Derived Black Carbon (Biochar) as a Microbial Electron Donor and Acceptor. *Environ. Sci. Technol. Lett.* **2016**, *3* (2), 62−66.
(30) Lehmann, J. A Handful of Carbon. *Nature* **2007**, *447* (7141), 143−144.
(31) Lehmann, J.; Gaunt, J.; Rondon, M. Bio-Char Sequestration in Terrestrial Ecosystems - A Review. *Mitigation and Adaptation Strategies for Global Change.* **2006**, *11*, 403−427.
(32) Sun, T.; Guzman, J. J. L.; Seward, J. D.; Enders, A.; Yavitt, J. B.; Lehmann, J.; Angenent, L. T. Suppressing Peatland Methane Production by Electron Snorkeling through Pyrogenic Carbon in Controlled Laboratory Incubations. *Nat. Commun.* **2021**, *12* (1), 4119 DOI: 10.1038/s41467-021-24350-y.
(33) Feng, Y.; Xu, Y.; Yu, Y.; Xie, Z.; Lin, X. Mechanisms of Biochar Decreasing Methane Emission from Chinese Paddy Soils. *Soil Biol. Biochem* **2012**, *46*, 80−88.
(34) Nan, Q.; Xin, L.; Qin, Y.; Waqas, M.; Wu, W. Exploring Long-Term Effects of Biochar on Mitigating Methane Emissions from Paddy Soil: A Review. *Biochar* **2021**, *3*, 125−134.
(35) Xin, D.; Xian, M.; Chiu, P. C. New Methods for Assessing Electron Storage Capacity and Redox Reversibility of Biochar. *Chemosphere* **2019**, *215*, 827−834.

(36) Bolyen, E.; Rideout, J. R.; Dillon, M. R.; Bokulich, N. A.; Abnet, C. C.; Al-Ghalith, G. A.; Alexander, H.; Alm, E. J.; Arumugam, M.; Asnicar, F.; Bai, Y.; Bisanz, J. E.; Bittinger, K.; Brejnrod, A.; Brislawn, C. J.; Brown, C. T.; Callahan, B. J.; Caraballo-Rodríguez, A. M.; Chase, J.; Cope, E. K.; Da Silva, R.; Diener, C.; Dorrestein, P. C.; Douglas, G. M.; Durall, D. M.; Duvallet, C.; Edwardson, C. F.; Ernst, M.; Estaki, M.; Fouquier, J.; Gauglitz, J. M.; Gibbons, S. M.; Gibson, D. L.; Gonzalez, A.; Gorlick, K.; Guo, J.; Hillmann, B.; Holmes, S.; Holste, H.; Huttenhower, C.; Huttley, G. A.; Janssen, S.; Jarmusch, A. K.; Jiang, L.; Kaehler, B. D.; Kang, K. Bin; Keefe, C. R.; Keim, P.; Kelley, S. T.; Knights, D.; Koester, I.; Kosciolek, T.; Kreps, J.; Langille, M. G. I.; Lee, J.; Ley, R.; Liu, Y. X.; Loftfield, E.; Lozupone, C.; Maher, M.; Marotz, C.; Martin, B. D.; McDonald, D.; McIver, L. J.; Melnik, A. V.; Metcalf, J. L.; Morgan, S. C.; Morton, J. T.; Naimey, A. T.; Navas-Molina, J. A.; Nothias, L. F.; Orchanian, S. B.; Pearson, T.; Peoples, S. L.; Petras, D.; Preuss, M. L.; Pruesse, E.; Rasmussen, L. B.; Rivers, A.; Robeson, M. S.; Rosenthal, P.; Segata, N.; Shaffer, M.; Shiffer, A.; Sinha, R.; Song, S. J.; Spear, J. R.; Swafford, A. D.; Thompson, L. R.; Torres, P. J.; Trinh, P.; Tripathi, A.; Turnbaugh, P. J.; Ul-Hasan, S.; van der Hooft, J. J. J.; Vargas, F.; Vázquez-Baeza, Y.; Vogtmann, E.; von Hippel, M.; Walters, W.; Wan, Y.; Wang, M.; Warren, J.; Weber, K. C.; Williamson, C. H. D.; Willis, A. D.; Xu, Z. Z.; Zaneveld, J. R.; Zhang, Y.; Zhu, Q.; Knight, R.; Caporaso, J. G. Reproducible, Interactive, Scalable and Extensible Microbiome Data Science Using QIIME 2. *Nat. Biotechnol.* **2019**, *37*, 852−857.

(37) Callahan, B. J.; McMurdie, P. J.; Rosen, M. J.; Han, A. W.; Johnson, A. J. A.; Holmes, S. P. DADA2: High-Resolution Sample Inference from Illumina Amplicon Data. *Nat. Methods* **2016**, *13* (7), 581−583.

(38) Yilmaz, P.; Parfrey, L. W.; Yarza, P.; Gerken, J.; Pruesse, E.; Quast, C.; Schweer, T.; Peplies, J.; Ludwig, W.; Glöckner, F. O. The SILVA and "All-Species Living Tree Project (LTP)" Taxonomic Frameworks. *Nucleic Acids Res.* **2014**, *42* (D1), D643−D648.

(39) Michelson, K.; Sanford, R. A.; Valocchi, A. J.; Werth, C. J. Nanowires of *Geobacter Sulfurreducens* Require Redox Cofactors to Reduce Metals in Pore Spaces Too Small for Cell Passage. *Environ. Sci. Technol.* **2017**, *51* (20), 11660−11668.

(40) Bai, Y.; Mellage, A.; Cirpka, O. A.; Sun, T.; Angenent, L. T.; Haderlein, S. B.; Kappler, A. AQDS and Redox-Active NOM Enables Microbial Fe(III)-Mineral Reduction at cm-Scales. *Environ. Sci. Technol.* **2020**, *54* (7), 4131−4139.

(41) Michelson, K.; Alcalde, R. E.; Sanford, R. A.; Valocchi, A. J.; Werth, C. J. Diffusion-Based Recycling of Flavins Allows Shewanella Oneidensis MR-1 to Yield Energy from Metal Reduction Across Physical Separations. *Environ. Sci. Technol.* **2019**, *53* (7), 3480−3487.

(42) Cheng, Q.; Call, D. F. Developing Microbial Communities Containing a High Abundance of Exoelectrogenic Microorganisms Using Activated Carbon Granules. *Sci. Total Environ.* **2021**, *768*, No. 144361.

(43) Wang, C.; Liu, Y.; Wang, C.; Xing, B.; Zhu, S.; Huang, J.; Xu, X.; Zhu, L. Biochar facilitates rapid restoration of methanogenesis by enhancing direct interspecies electron transfer after high organic loading shock. *Bioresour. Technol.* **2021**, *320*, No. 124360.

(44) Gao, J.; Liu, L.; Shi, Z.; Lv, J. Biochar Amendments Facilitate Methane Production by Regulating the Abundances of Methanogens and Methanotrophs in Flooded Paddy Soil. *Front. soil sci* **2022**, *2*, No. 801227.

(45) Pan, J.; Ma, J.; Liu, X.; Zhai, L.; Ouyang, X.; Liu, H. Effects of different types of biochar on the anaerobic digestion of chicken manure. *Bioresour. Technol.* **2019**, *275*, 258−265.

(46) Chen, S.; Rotaru, A.-E.; Liu, F.; Philips, J.; Woodard, T. L.; Nevin, K. P.; Lovley, D. R. Carbon Cloth Stimulates Direct Interspecies Electron Transfer in Syntrophic Co-Cultures. *Bioresour. Technol.* **2014**, *173*, 82−86.

(47) Chen, S.; Rotaru, A.-E.; Shrestha, P. M.; Malvankar, N. S.; Liu, F.; Fan, W.; Nevin, K. P.; Lovley, D. R. Promoting Interspecies Electron Transfer with Biochar. *Sci. Rep.* **2014**, *4* (1), 5019.

(48) Dang, Y.; Holmes, D. E.; Zhao, Z.; Woodard, T. L.; Zhang, Y.; Sun, D.; Wang, L.-Y.; Nevin, K. P.; Lovley, D. R. Enhancing Anaerobic Digestion of Complex Organic Waste with Carbon-Based Conductive Materials. *Bioresour. Technol.* **2016**, *220*, 516−522.

(49) Zhao, Z.; Zhang, Y.; Woodard, T. L.; Nevin, K. P.; Lovley, D.R. Enhancing Syntrophic Metabolism in Up-Flow Anaerobic Sludge Blanket Reactors with Conductive Carbon Materials. *Bioresour. Technol.* **2015**, *191*, 140−145.

(50) Rush, J. E.; Zalman, C. A.; Woerndle, G.; Hanna, E. L.; Bridgham, S. D.; Keller, J. K. Warming promotes the use of organic matter as an electron acceptor in a peatland. *Geoderma* **2021**, *401*, No. 115303.

(51) Soued, C.; Harrison, J. A.; Mercier-Blais, S.; Prairie, Y. T. Reservoir CO_2 and CH_4 Emissions and Their Climate Impact over the Period 1900−2060. *Nat. Geosci* **2022**, *15*, 700.

(52) IPCC *Climate Change 2022: Mitigation of Climate Change: Contribution of Working Group III to the Sixth Assessment Report of the Intergovernmental Panel on Climate Change*; Cambridge University Press, 2023; DOI: 10.1017/9781009157926.

(53) Williams, A. P.; Abatzoglou, J. T.; Gershunov, A.; Guzman-Morales, J.; Bishop, D. A.; Balch, J. K.; Lettenmaier, D. P. Observed Impacts of Anthropogenic Climate Change on Wildfire in California. *Earths Future* **2019**, *7* (8), 892−910.

(54) Zimmerman, A. R.; Mitra, S. Trial by Fire: On the Terminology and Methods Used in Pyrogenic Organic Carbon Research. *Front. Earth Sci. (Lausanne)* **2017**, *5*, 95 DOI: 10.3389/feart.2017.00095.

(55) Lehmann, J. A Handful of Carbon. *Nature* **2007**, *447* (7141), 143−144.

(56) Lehmann, J.; Gaunt, J.; Rondon, M. Bio-Char Sequestration in Terrestrial Ecosystems - A Review. *Mitigation and Adaptation Strategies for Global Change* **2006**, *11*, 403−427.

(57) Molina, M.; Zaelke, D.; Sarma, K. M.; Andersen, S. O.; Ramanathan, V.; Kaniaru, D. Reducing Abrupt Climate Change Risk Using the Montreal Protocol and Other Regulatory Actions to Complement Cuts in CO_2 Emissions. *Proc. Natl. Acad. Sci. U. S. A.* **2009**, *106* (49), 20616−20621.

NOTE ADDED AFTER ASAP PUBLICATION

This paper was published ASAP on December 1, 2023, with the wrong Supporting Information file. The corrected version was reposted on December 12, 2023.

https://doi.org/10.1021/acs.est.3c05830
Environ. Sci. Technol. 2023, 57, 20605−20614